Channel-Facilitated Diffusion Boosted by Particle Binding at the Channel Entrance

Stefano Pagliara,[*] Simon L. Dettmer,[†] and Ulrich F. Keyser[‡]

Cavendish Laboratory, CB30HE Cambridge, United Kingdom

We investigate single-file diffusion of Brownian particles in arrays of closely confining microchannels permeated by a variety of attractive optical potentials and connecting two baths with equal particle concentration. We simultaneously test free diffusion in the channel, diffusion in optical traps coupled in the center of the channel, and diffusion in traps extending into the baths. We found that both classes of attractive optical potentials enhance the translocation rate through the channel with respect to free diffusion. Surprisingly, for the latter class of potentials we measure a 40-fold enhancement in the translocation rate with respect to free diffusion and find a sublinear power law dependence of the translocation rate on the average number of particles in the channel. Our results reveal the function of particle binding at the channel entrances for diffusive transport and open the way to a better understanding of membrane transport and design of synthetic membranes with enhanced diffusion rate.

Particle transport through membrane channels and pores that connect three-dimensional (3D) compartmentalized environments, represents a crucial step in a variety of biological, physical, and chemical processes [1–3]. Such channels often exhibit binding sites specific for the transported particles and the binding strength can be optimized in order to maximize the particle transport thus exceeding the one in a nonbinding channel [4]. This has been extensively investigated experimentally [5–8], by molecular dynamics simulations [9], and independently rationalized by a continuum diffusion model based on the Smoluchowski equation [10], a discrete stochastic model [11], a generalized macroscopic version of Fick's diffusion law [12], and a general kinetic model [13].

Binding sites are also found close to the entrances of membrane channels where these might play a key role in the so-called entrance effects [14]. Examples are found in various biological systems as follows. (i) The channel maltoporin, found in gram-negative bacteria, presenting sugar-affine aromatic residues, both at the entrance vestibule and at the exit to the periplasmic side [15,16]. (ii) The outer membrane channel OmpF of *Escherichia coli* exhibiting two symmetric binding sites for fluoroquinolone antibiotics located at each channel entry separated by a large energy barrier in the center [17]. (iii) The nuclear pore complexes of eukaryotic cells presenting docking sites both at the basket structure on the nuclear face and on fibrils in the cytoplasmic side [18,19]. (iv) On the membrane of leukocytes, epithelial, and endothelial cells where they are exploited by bacterial toxins to form pores in lipid bilayers [20,21].

Despite being involved in antibiotic resistance [17] and bacterial and viral invasion [20,22], the function and role of such docking and binding sites at the channel entrances or in their proximity often remain elusive [16] since it is notoriously difficult, on one hand, to arrive at analytical

expressions to model their influence on the molecular transport, and, on the other hand, to experimentally control the position and strength of such sites. Together with theoretical modeling [23–25], colloidal particles in microfluidics [26–29] equipped with holographic optical tweezers (HOTs) [30–33] and digital video microscopy [34] allow us to investigate constrained Brownian motion in quasi one-dimensional (1D) structures and to build experimental model systems to mimic transport properties of biological channels [35–38].

In this Letter we investigate single-file diffusion of Brownian particles in an array of closely confining microchannels permeated by a variety of attractive optical potentials realized via HOTs. Specifically, we simultaneously test transport properties of particles diffusing in laser-free channels, channels permeated by internal optical potentials, and channels permeated by potentials that extend into the baths [Fig. 1(a)]. We use focused ion beam, photolithography, replica molding, and oxygen plasma bonding to fabricate microfluidic chips equipped with arrays of parallel channels that connect two 3D baths otherwise separated by a polydimethylsiloxane barrier [Fig. 1(b)] [39]. The channels have a length $l = 4.5$ μm and a semielliptical cross section with both height h and width w around 950 nm. The maximum variation among the channel widths and heights is less than 5% and 10%, respectively, as measured by scanning electron microscopy. The baths, which have a depth of 16 μm, are filled with a suspension of polystyrene spherical particles with diameter $d = (505 \pm 8)$ nm in a 5 mM KCl solution. The particle concentration is 0.05 μm^{-3} in both baths. Particles freely diffuse in the 3D baths while being closely confined and in single file diffusion in the microfluidic channels. We use a custom made HOTs setup consisting of an inverted microscope equipped with an ytterbium fiber laser, a phase only spatial light modulator
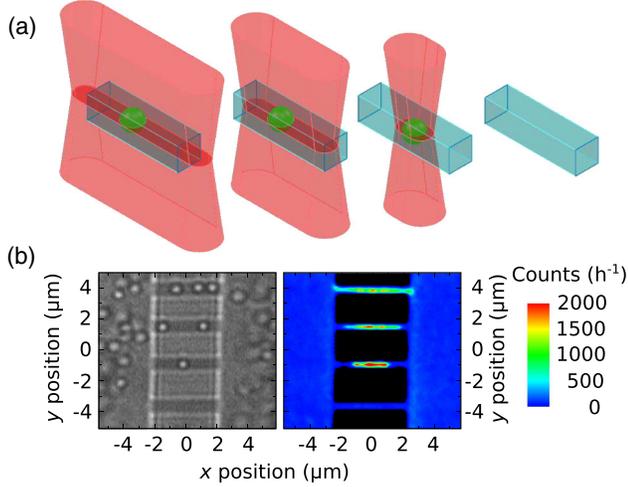
FIG. 1 (color online). Array of microfluidic channels with different energy landscapes. (a) Scheme of an array of laser traps generated via holographic optical tweezers and coupled into microfluidic channels that create independent attractive energy landscapes for Brownian particles. (b) Bright field image (left) and corresponding map of the number of particle occurrences (per bin and per hour, right) of four microfluidic channels with similar dimensions connecting two 3D baths. The baths have a depth of $16\,\mu m$. The spherical particles have a diameter (505 ± 8) nm. Laser line traps are coupled in each channel occupying, 5/4, 1, 1/2, and 0 of the channel length from top to bottom, respectively. The total coupled laser power is 900 mW and we programmed the SLM to generate the 3 lines with a relative intensity of 1, 0.7, and 0.6 from top to bottom, respectively.

(SLM), a high magnification objective ($100\times$, 1.4 NA), a CCD camera, and a xyz nanopositioning piezo stage [35]. We couple line traps of a specific length in different channels and define $\lambda = L/l$ as the ratio between the laser line length L and the channel length l.

In the bright field image in Fig. 1(b) the top three channels are coupled with 3 laser lines with $\lambda \approx 5/4$, 1, 1/2 (from top to bottom) while no laser is coupled in the lowest channel ($\lambda = 0$) where particles are in free diffusion. The corresponding attractive energy profiles per particle $u(x)$ are reported in Fig. S1(a) of the Supplemental Material [40]. The average potential depth, U, linearly scales with P/L [Fig. S1(b)] as expected, confirming that the laser lines act as attractive potential wells [35,41]. We track the particle positions at all time both in the channels and in the baths [42]. Particle counts are typically below 100 h^{-1} (blue) in the baths and in the lowest channel while they go up to 1000–2000 h^{-1} (green and red) in the top three channels. The particle diffusion coefficients in the channel D_C and in the bath D_B—measured as previously reported [43]—do not exhibit any significant dependence on the laser power (Fig. S7 in the Supplemental Material [40]) suggesting that the particle motion is not affected by laser induced heating.

We define an attempt as the event for which a particle enters into the channel from either bath and explores it for
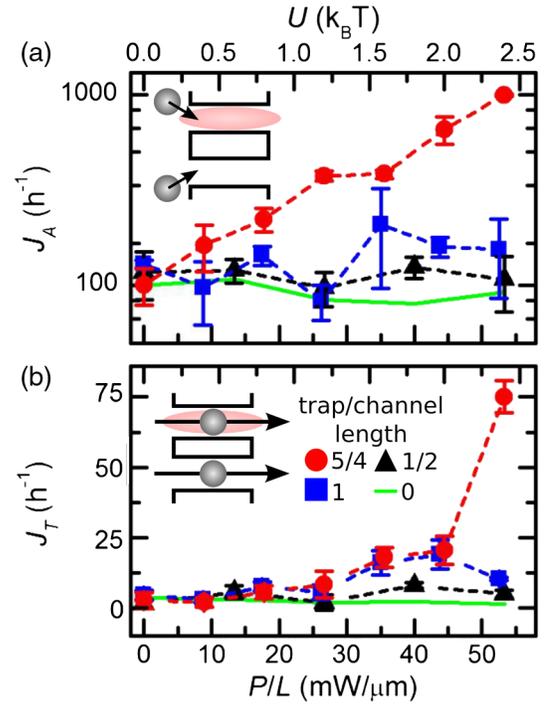
FIG. 2 (color online). Comparison of transport through channels with shallow internal and external attractive potentials. Dependence of J_A (a), and J_T (b) on P/L (bottom axis) and U (top axis) for $\lambda \approx 5/4$ (circles), 1 (squares), 1/2 (upward triangles), and 0 (solid line). Each data point and corresponding error bar are the mean and standard deviation of three independent measurements lasting 1 h. Lines are guides for the eye. The solid lines connect the seven data points for the channel in free diffusion; error bars are omitted. The three optical line traps are coupled in a different channel in every video. The total applied power is randomized to cover 7 discrete steps from 0 to 900 mW. Insets: illustration of an attempt (a) and a translocation (b) in two different channels, the top with a coupled laser line, the bottom in free diffusion.

at least 100 ms [inset Fig. 2(a)] [35]. The same particle may enter and exit the channel multiple times. Once a particle has entered the channel, it can either go back to the same bath, defined as return event, or translocate the channel and exit to the opposite bath, defined as translocation event [inset Fig. 2(b)]. We characterize the transport in the investigated energy landscapes in terms of attempt rate J_A, translocation rate J_T, and translocation probability $p_T = J_T/J_A$. In addition, we quantify the probabilities to find n particles in the channel $p(n)$ and the average number of particles in the channel N.

J_A stays constant around 100 h^{-1} both for $\lambda = 0$ and 1/2 [solid line and upward triangles in Fig. 2(a), respectively], and increases up to 200 h^{-1} for $\lambda \approx 1$ (squares). Importantly, J_A monotonically increases with P/L up to 1000 h^{-1} for 50 mW/μm and $\lambda \approx 5/4$ (circles). In free diffusion there is at most one particle in the channel and p_T can be predicted as [44]

$$p_T = \frac{1}{2 + \frac{4D_B l}{\pi D_C a}}, \qquad (1)$$

where the effective radius of the channel is $a = (h-d)/2 = 0.22$ μm. By using the experimental parameters obtained from our measurements we predict $p_T = 0.013$. We test free diffusion in 30 different repeats, 12 times in 4 different channels when the laser is off and 18 times in a reference channel when the laser is on, with an average $p_T = (0.022 \pm 0.003)$. The constant monitoring of free diffusion is crucial for the continuous assessment of Brownian motion [42]. The measured probability is larger than predicted which presumably stems from our definition of an attempt (see above) and thus we do not count very short events. In the channels permeated by the optical traps $p(n > 1)$ is nonnegligible (Fig. S4 in the Supplemental Material [40]) and thus the current set of data cannot be described by theoretical models based on a single particle picture. For internal traps the dependence of J_T on P/L is nonmonotonic with a peak that is 4 [$\lambda \approx 1/2$, triangles in Fig. 2(b)] and 10 times ($\lambda \approx 1$, squares) larger with respect to the free diffusion case (solid line). On the contrary, external line traps ($\lambda \approx 5/4$) produce a monotonic increase in J_T up to 75 h^{-1} for the highest applied power which produces an attractive potential of average depth $U \approx 2.5k_BT$.

We perform additional experiments with $\lambda \approx 5/4$ and P/L above 50 mW/μm while keeping a reference channel in free diffusion. The particle concentration c is lowered to 0.015 μm^{-3} in order to avoid the jamming of the channel, which is populated by up to seven particles—in single file diffusion—at high laser powers (Fig. S5 in the Supplemental Material [40]). We measure a mean J_A for free diffusion of (38 ± 2) h^{-1} (obtained as the mean and standard error of the mean of 36 measurements). J_A can be predicted according to the expression for the rate constant for an elliptical aperture k_0 [45],

$$J_A = 2k_0 c = 2D_B \frac{1}{2} \sqrt[3]{\frac{32AP}{\pi}} c, \qquad (2)$$

where A and P are the area and perimeter of the ellipse, respectively, 2 accounts for both apertures of the channel and 1/2 for the semielliptical shape. By using the experimental parameters determined from our measurements we find $J_A = 52$ h^{-1}. This value is higher with respect to the measured one that presumably stems from our definition of an attempt (see above) and thus we do not count very short events. Consistent with the data reported in Fig. 2, for $\lambda \approx 5/4$ J_A monotonically increases up to 5500 h^{-1} for $P/L \approx 105$ mW/μm [circles in Fig. 3(a)] but decreases for higher laser powers as discussed in the Supplemental Material [40]. $\lambda \approx 5/4$ produces an enhancement in J_A of more than 2 orders of magnitude with respect to free diffusion. A simple way to rationalize this effect is by considering that the laser generates a 3D particle absorber
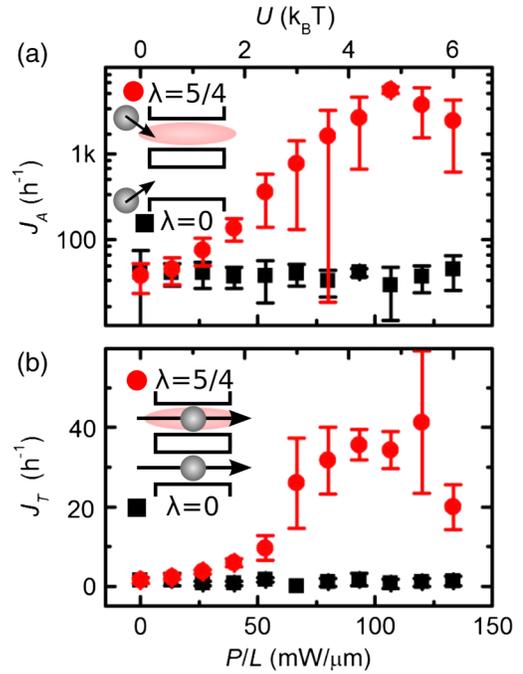
FIG. 3 (color online). Transport enhancement through channels with deeper external attractive potentials. (a) J_A and (b) J_T as a function of P/L (bottom axis) and U (top axis) for $\lambda \approx 5/4$ (circles). The transport through the channel with the attractive potential is compared with the one through a channel in free diffusion ($\lambda = 0$, squares). Each data point and corresponding error bar are the mean and standard deviation of three independent measurements.

in the bath. In first approximation we can model this absorber as a sphere with diameter R equal to the extension in the bath of the attractive potential [Fig. S2(a) in the Supplemental Material [40]]. Similarly to U, also R linearly increases with the applied laser power up to 1 μm for the highest power [Fig. S2(b)]. According to the expression of the rate constant for a spherical absorber k_1 [46], the attempt rate is predicted as

$$J_A = 2k_1 c = 2\left(4\pi D_B \frac{R}{2}\right)c, \qquad (3)$$

where 2 accounts for the two baths. By using the experimental parameters determined from our measurements for the highest laser power, we find a predicted $J_A > 500$ h^{-1}, thus 1 order of magnitude higher with respect to the one predicted for free diffusion. The measured J_A is higher since we do not measure the number of particles captured in the sphere but rather their multiple attempts to enter the channel.

Consistent with the data reported in Fig. 2, the increase in J_A produces, in turn, an enhancement in J_T [Fig. 3(b)]. While $J_T = 1$ h^{-1} in free diffusion, for $\lambda \approx 5/4$ $J_{T, \text{Max}} = 40$ h^{-1} for $P/L = 120$ mW/μm and $U \approx 5.5k_BT$. Moreover, a threefold increase in J_T is observed for P/L between 55 and 65 mW/μm, consistent with the data reported in Fig. 2(b). This further reflects the enhancement in the
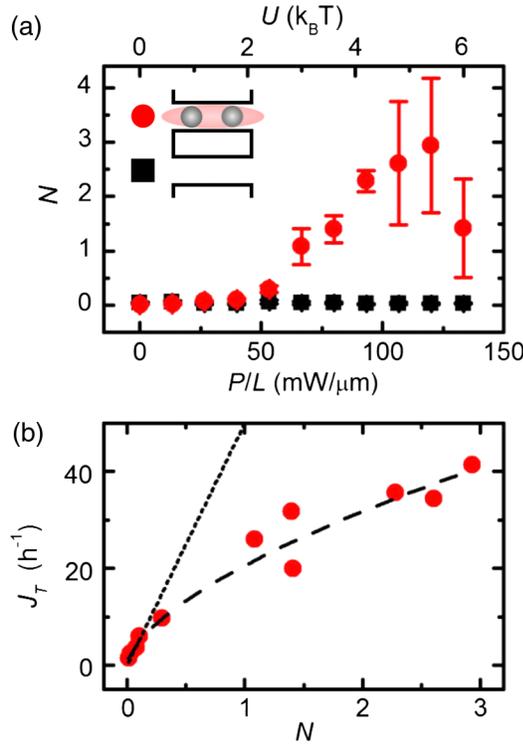
FIG. 4 (color online).   Correlation between translocation rate and particle number. (a) Dependence of N on P/L (bottom axis) and U (top axis) for $\lambda \approx 5/4$ (circles) and comparison with a control channel in free diffusion ($\lambda = 0$, squares). Each data point and corresponding error bar are the mean and standard deviation of three independent measurements. (b) Correlation between J_T and N. Error bars are reported in (a) and Fig. 3(b). The dotted line is a linear fit of the first 4 points in the graph with the intercept forced to zero. The dashed line is a sublinear power law fit of the whole data set with the intercept forced to zero.

measured occupation probability in Fig. S5: $p(n = 0)$ drastically decreases from 0.73 to 0.38 for P/L between 55 and 65 mW/μm while $p(n = 1)$, $p(n = 2)$, and $p(n = 3)$ become 2, 8, and 30 times larger, respectively. Importantly, the remarkable enhancement in J_T is due to a different mechanism with respect to the one reported for internal optical traps: for internal potentials p_T increases up to 0.12 [Fig. S6(a) in the Supplemental Material [40]], for the external ones p_T decreases down to a minimum of 0.006 [Fig. S6(b) in the Supplemental Material [40]]. Nevertheless, the enhancement in J_A, boosts J_T up to a value 40 times higher with respect to free diffusion.

Moreover, it is noteworthy that also N increases with P/L [Fig. 4(a)]. Figure 4(b) shows that J_T linearly increases with N for small occupancies ($N \ll 1$). Indeed, in the limit of single particle occupancy J_T is proportional to N [47] [provided that the variation of the translocation probability is negligible, which is the case here, see data for $15 < P/L < 40$ mW/μm in Fig. S6(b)]. A linear fit of the first four points forcing the intercept to 0 gives a slope of 50 h^{-1} [dotted line in Fig. 4(b)]. However, we measure

$J_T = 25$ h^{-1} for $N = 1$. Therefore, a linear dependence fails in describing multiparticle diffusion, similarly to recent studies on alkali and alkali earth ion transport in molecular pores [47]. On the contrary, the entire set of data can be described by a sublinear power law [dashed line in Fig. 4(b)],

$$J_T = aN^b, \tag{4}$$

which gives $a = (21 \pm 1)$ and $b = (0.62 \pm 0.02)$ as fitting parameters. The sublinear power law can be understood with the following consideration: multiple particles entering the channel from two opposite baths compete for success and not all of them can translocate.

These experimental observations allow us to draw some conclusions. (i) In the presented 3D-1D-3D environments, that are ubiquitous in nature, the closely confining channels represent the rate limiting step in particle exchange being empty for more than 98% of the time and leading to $J_T = 1$ h^{-1}. (ii) Attractive potentials localized inside the channel increase both N and p_T and enhance J_T up to 10 times compared to free diffusion. (iii) A similar enhancement is observed for shallow optical potentials ($U \approx 2k_BT$) that extend into the baths for less than one particle diameter. (iv) Deeper external potentials, extending in the baths for more than one particle diameter, allow for up to 40 times enhancement in J_T with respect to free diffusion. (v) In the general case of equal concentration of particles in the 3D baths and in the presence of potentials that extend into the baths, the competition for channel translocation between particles entering from opposite baths leads to a sublinear power law correlation between J_T and N.

These findings demonstrate that not only the strength but also the extension and position of the interaction between the transported particle and the transporter channel are crucial in facilitating diffusion. Our findings could guide the design of more efficient synthetic membranes relevant for catalysis, osmosis, and particle separation and help in modeling transport phenomena, chemical kinetics, protein folding, and enzymatic reactions [48–51].

[*]sp608@cam.ac.uk
[†]Present address: Institute for Theoretical Physics, University of Cologne, Zülpicher Strasse 77, D-50937 Cologne, Germany.
[‡]ufk20@cam.ac.uk
[1] T. Chou and D. Lohse, Phys. Rev. Lett. **82**, 3552 (1999).

[2] M. Muthukumar, *Polymer Translocation* (CRC Press, Boca Raton, 2011).
[3] P. Hanggi and F. Marchesoni, Rev. Mod. Phys. **81**, 387 (2009).
[4] J. J. Kasianowicz, T. L. Nguyen, and V. M. Stanford, Proc. Natl. Acad. Sci. U.S.A. **103**, 11431 (2006).
[5] M. Luckey and H. Nikaido, Proc. Natl. Acad. Sci. U.S.A. **77**, 167 (1980).
[6] J. E. W. Meyer and G. E. Schulz, Protein Sci. **6**, 1084 (1997).
[7] R. Benz, A. Schmid, T. Nakae, and G. H. Vos-Scherperkeuter, J. Bacteriol. **165**, 978 (1986).
[8] L. Kullman, M. Winterhalter, and S. M. Bezrukov, Biophys. J. **82**, 803 (2002).
[9] M. O. Jensen, S. Park, E. Tajkhorshid, and K. Schulten, Proc. Natl. Acad. Sci. U.S.A. **99**, 6731 (2002).
[10] A. M. Berezhkovskii and S. M. Bezrukov, Biophys. J. **88**, L17 (2005).
[11] A. B. Kolomeisky, Phys. Rev. Lett. **98**, 048105 (2007).
[12] W. R. Bauer and W. Nadler, Proc. Natl. Acad. Sci. U.S.A. **103**, 11446 (2006).
[13] A. Zilman, Biophys. J. **96**, 1235 (2009).
[14] S. Gravelle, L. Joly, F. Detcheverry, C. Ybert, C. Cottin-Bizonne, and L. Bocquet, Proc. Natl. Acad. Sci. U.S.A. **110**, 16367 (2013).
[15] R. Dutzler, Y. F. Wang, P. J. Rizkallah, J. P. Rosenbusch, and T. Schirmer, Structure **4**, 127 (1996).
[16] C. Hilty and M. Winterhalter, Phys. Rev. Lett. **86**, 5624 (2001).
[17] K. R. Mahendran, E. Hajjar, T. Mach, M. Lovelle, A. Kumar, I. Sousa, E. Spiga, H. Weingart, P. Gameiro, M. Winterhalter, and M. Ceccarelli, J. Phys. Chem. B **114**, 5170 (2010).
[18] I. G. Macara, Microbiol. Mol. Biol. Rev. **65**, 570 (2001).
[19] C. Strambio-De-Castillia, M. Niepel, and M. P. Rout, Nat. Rev. Mol. Cell Biol. **11**, 490 (2010).
[20] J. A. T. Young and R. J. Collier, Annu. Rev. Biochem. **76**, 243 (2007).
[21] S. Johnson, N. J. Brooks, R. A. Smith, S. M. Lea, and D. Bubeck, Cell Rep. **3**, 1369 (2013).
[22] A. A. Labokha and A. Fassati, Viruses **5**, 2410 (2013).
[23] D. Reguera, G. Schmid, P. S. Burada, J. M. Rubí, P. Reimann, and P. Hänggi, Phys. Rev. Lett. **96**, 130603 (2006).
[24] P. Reimann, C. Van den Broeck, H. Linke, P. Hänggi, J. M. Rubi, and A. Pérez-Madrid, Phys. Rev. Lett. **87**, 010602 (2001).
[25] S. Martens, A. V. Straube, G. Schmid, L. Schimansky-Geier, and P. Hänggi, Phys. Rev. Lett. **110**, 010601 (2013).
[26] X. Xu, B. Lin, B. Cui, A. R. Dinner, and S. A. Rice, J. Chem. Phys. **132**, 084902 (2010).
[27] E. Wonder, B. Lin, and S. A. Rice, Phys. Rev. E **84**, 041403 (2011).
[28] B. Lin, B. Cui, X. Xu, R. Zangi, H. Diamant, and S. A. Rice, Phys. Rev. E **89**, 022303 (2014).
[29] S. Bleil, P. Reimann, and C. Bechinger, Phys. Rev. E **75**, 031117 (2007).
[30] J. E. Curtis, B. A. Koss, and D. G. Grier, Opt. Commun. **207**, 169 (2002).
[31] D. Grier, Nature (London) **424**, 810 (2003).
[32] M. Padgett and R. Bowman, Nat. Photonics **5**, 343 (2011).
[33] M. Padgett and R. Di Leonardo, Lab Chip **11**, 1196 (2011).
[34] J. C. Crocker and D. G. Grier, J. Colloid Interface Sci. **179**, 298 (1996).
[35] S. Pagliara, C. Schwall, and U. F. Keyser, Adv. Mater. **25**, 844 (2013).
[36] Y. Caspi, D. Zbaida, H. Cohen, and M. Elbaum, Nano Lett. **8**, 3728 (2008).
[37] S. W. Kowalczyk, L. Kapinos, T. R. Blosser, T. Magalhaes, P. van Nies, R. Y. H. Lim, and C. Dekker, Nat. Nanotechnol. **6**, 433 (2011).
[38] S. W. Kowalczyk, T. R. Blosser, and C. Dekker, Trends Biotechnol. **29**, 607 (2011).
[39] S. Pagliara, C. Chimerel, R. Langford, D. G. A. L. Aarts, and U. F. Keyser, Lab Chip **11**, 3365 (2011).
[40] See Supplemental Material at http://link.aps.org/supplemental/10.1103/PhysRevLett.113.048102 for detailed evaluation of the optical potential profiles, the channel occupation and translocation probabilities, and the particle diffusion coefficients in the baths and in the channels..
[41] M. Polin, Y. Roichman, and D. G. Grier, Phys. Rev. E **77**, 051401 (2008).
[42] S. L. Dettmer, U. F. Keyser, and S. Pagliara, Rev. Sci. Instrum. **85**, 023708 (2014).
[43] S. L. Dettmer, S. Pagliara, K. Misiunas, and U. F. Keyser, Phys. Rev. E **89**, 062305 (2014).
[44] A. M. Berezhkovskii, M. A. Pustovoit, and S. M. Bezrukov, J. Chem. Phys. **116**, 9952 (2002).
[45] O. Dudko, A. Berezhkovskii, and G. Weiss, J. Chem. Phys. **121**, 1562 (2004).
[46] H. Berg and E. Purcell, Biophys. J. **20**, 193 (1977).
[47] I. Kaufman, D. G. Luchinsky, R. Tindjong, P. V. E. McClintock, and R. S. Eisenberg, Phys. Rev. E **88**, 052712 (2013).
[48] P. C. Bressloff and J. M. Newby, Rev. Mod. Phys. **85**, 135 (2013).
[49] A. M. Berezhkovskii, A. Szabo, and H.-X. Zhou, J. Chem. Phys. **135**, 075103 (2011).
[50] H.-X. Zhou and J. A. McCammon, Trends Biochem. Sci. **35**, 179 (2010).
[51] E. C. Yusko, J. M. Johnson, S. Majd, P. Prangkio, R. C. Rollings, J. Li, J. Yang, and M. Mayer, Nat. Nanotechnol. **6**, 253 (2011).